International Journal of Thermophysics, Vol. 10, No. 2, 1989

Absolute Absorptance Measurements on Copper-Based Allows at Infrared Wavelengths[1]

R. Webb[2]

We report on a method for obtaining absolute optical absorptance of a metallic sample whereby thermal equilibrium is maintained by balancing input from a laser beam with thermoelectric cooling. This method was applied to a series of copperbased alloy samples and was performed at 1.06 and 10.6 μm using continuous Nd:YAG and CO_2 laser sources, respectively, at near-normal (6°) incidence to the sample faces. Independent calibration was provided by passing a known current through a standard resistance heater. Precision of the technique was demonstrated to be within 5% for all samples. Comparison of experimentally derived absorptance values with DC electrical resistivity yielded rank ordering of data for the 20 sample alloys measured.

KEY WORDS: copper-based alloys; infrared laser measurements; metallic optics; optical absorptance; radiative properties.

1. INTRODUCTION

We present a method for measuring the absolute optical absorptance of a metallic sample. The method is based upon offsetting the power from a continuously impinging laser beam by an equal amount of cooling power produced by a set of Peltier junctions. The net effect is to maintain the face of the specimen sample opposite to that of the impinging beam at its original temperature, thus preserving thermal equilibrium while monitoring the power delivered to the Peltier cooler. The latter is independently calibrated by passing a known current through a fixed resistance heater. By measuring power to the Peltier junctions as a function of laser input power, a linear relationship is observed over an adjustable range.

[1] Paper presented at the Tenth Symposium on Thermophysical Properties, June 20–23, 1988, Gaithersburg, Maryland, U.S.A.

[2] AT&T Engineering Research Center, Princeton, New Jersey 08540, U.S.A.

0195-928X/89/0300-0513$06.00/0

A least-squares fit to measured data was performed for 20 separate copper-based alloy samples. The slope of the linear fit to data yielded direct determinations of absolute absorptance. Results for these 20 samples were measured at two infrared wavelengths using two lasers, namely, Nd:YAG operating at 1.06 μm and CO_2 operating at 10.6 μm, and are reported below.

2. DESCRIPTION OF THE METHOD

We assume that the energy absorbed by the alloy is converted into heat, but a very small temperature rise takes place within the sample coupon. Furthermore, since we are dealing with copper-based alloys, which are good heat conductors, the time required for thermal diffusion throughout the sample is very short. We enclose the sample in vacuum to assure that no heat transfer takes place by convection; and since we limit the temperature rise to a negligible value above ambient, we further assume no energy loss due to radiation.

We attach the rear face of a given sample coupon to the top face of a two-stage Peltier thermoelectric cooler by means of thermally conductive grease. This interface thus provides the only means by which the sample coupon may lose its heat due to thermal conduction, while its polished optical face receives power from an impinging laser beam. The laser beam is maintained at a stable, continuous power level at an angle of incidence of 6° upon the coupon face, while the Peltier cooler current is adjusted to compensate for the heating effect of the laser beam in order to keep the rear coupon face temperature at equilibrium. Since we permit only a small amount of laser heating of the sample, the equilibrium temperature at the coupon/cooler interface is never allowed to deviate substantially from its initial temperature value. The current required to achieve such equilibrium is independently calibrated by means of a known resistance through which a carefully monitored current is passed to cause a computed amount of heat to be delivered to the Peltier cooler. Therefore, the current to the Peltier cooler establishes an absolute reference with respect to optical absorptance of the incident laser neam whose incident power level has been independently determined. That is, we are not measuring absorptance simply by monitoring reflected laser power. Instead, we are separately measuring the absolute amount of heat continuously generated within the sample coupon. This technique has special merit when measuring very small values of absorptance for very highly reflecting metallic samples where the optical power in the reflected beam is nearly equal to that of the incident beam itself.

3. EXPERIMENTAL APPARATUS

The quantity of heat removed at a set of Peltier junctions is proportional to the current passing through them. We utilize this effect to maintain a common side of such a set of Peltier junctions at a fixed initial temperature when the heat load is due to optical absorptance of a metal sample which is exposed to an input laser beam of a given wavelength. The metallic sample consists of a flat disk kept in intimate thermal contact with the Peltier device at one face, while the other face is exposed to the impinging laser beam at near-normal incidence at its opposite face.

It is recognized that the surface texture, oxidation condition, and degree of optical flatness are among the factors which influence the amount of absorptance with respect to the laser beam. Furthermore, all of the above factors limit the repeatability of measurements for a given metal or alloy type. Therefore we have selected samples that have been subjected to a series of grinding and polishing operations, which we have found to be repeatable within our laboratory. However, the technique itself is completely amenable to samples of any type and surface condition, provided they are compatible with the geometry of the apparatus. We simply restricted our own set of measurements, which are reported in this paper, to those made upon specimen samples with a degree of flatness, polish, and surface finish that we found to be repeatable.

We verified that it is not possible to perform absorptance measurements utilizing the Peltier coller technique described herein unless the sample is placed in an evacuated chamber. This is due primarily to convective air currents which cause the baseline temperature at the sample/junction device interface to wander substantially during the approximate half-day measurement per sample. Therefore, we constructed a special vacuum chamber which permits sample specimens to be inserted at a repeatable position within a few minutes' time. The removable vacuum sealed cover section contains a doubly antireflection-coated optical flat which serves as a window port. Two window materials were selected: zinc selenide for use with a CO_2 laser at a 10.6-μm and fused silica for use with a Nd:YAG laser at a 1.06-μm operating wavelength.

The Peltier cooler itself comprises two stages of junctions operated in series with respect to externally applied electric current. Specifically, we use a Model TS-801-1080-01 cooler manufactured by Cambridge Thermionic Corporation, selected because of its overall physical size and surface area of its cold junction face. This was thermally bonded to the massive aluminum heat sink built into the base of the vacuum chamber. The latter in turn was thermally bonded to the steel optical bench that was held at

a fixed ambient laboratory temperature, which is maintained throughout the year at 20°C within ±2°C.

Two continuous laser sources were used in our experimental measurements. One was a Quantronix Model 114 Nd:YAG laser operating at a 1.06-μm wavelength, producing a nominal 5 W of optical power within a 2-mm-diameter beam of approximately 2-mrad full angular divergence. The other was a Spectra Physics Model 941 CO_2 laser which produced a nominal 2 W of power at a 10.6-μm wavelength, also within a beam of 2-mm diameter and 2-mrad beam divergence. These two lasers were selected to have nearly identical beam characteristics and were run at fixed power levels chosen near their most stable operating points. Sets of fixed optical attenuators were used to vary the input optical power to the absorptance measurement chamber, rather than to vary the laser power directly. Again, this approach was selected in order to allow the lasers to operate at their most stable operating points throughout the entire series of measurements. Figure 1 shows that schematic arrangement of the apparatus used in this study. The laser power meter is shown in its reflected power monitoring position. However, it was swung into direct line with the optic axis of the laser to monitor the incident beam passing through the optical attenuators whenever incident power to the sample specimen was altered.

4. SAMPLE PREPARATION

Sheet stock of copper-based alloy samples was obtained from several commercial sources for all measurements made in this study. Compositions of all alloy samples were analyzed and are listed in Table I. Thicknesses

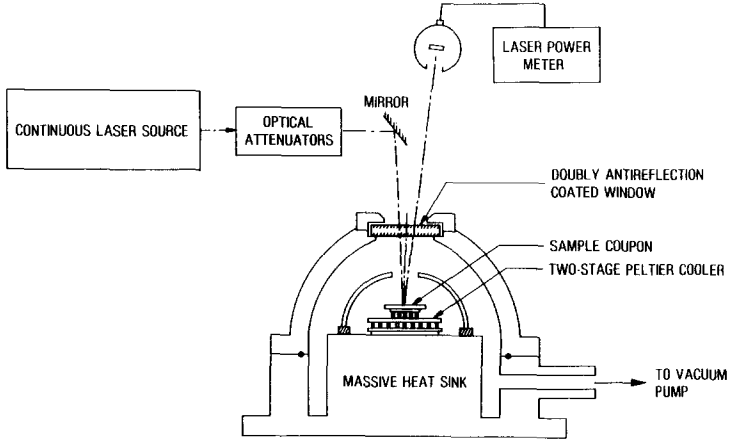

Fig. 1. Schematic arrangement of the measurement apparatus.

Table I. Copper-Base Alloy Specimen Composition

Sample No.	Alloy	Common name	Cu	Ni	Sn	Zn	Fe	Mn	As	P	Al	Cr	Si	Ag	Pb
1	C101	O_2 free Cu, Electronic	99.99												
2	C114	Tough pitch Cu w. Ag	99.92											0.03	
3	C122	High-residual P:Cu	99.9							0.04					
4	C182	Chromium-copper	99.21				0.07					0.68	0.01		
5	C230	Red brass	85.38			14.6	0.002								0.002
6	C260	Cartridge brass	70.5			29.5									
7	C443	Admiralty As:Cu	71.8		1.1	27.0			0.07						
8	C510	Phosphor bronze-A	95.43		4.42	0.06				0.06					
9	C521	Phosphor bronze-C	91.95		7.71	0.10				0.13					
10	C524	Phosphor bronze-D	89.9		9.71	0.20				0.23					
11	C608	Aluminum bronze	94.5			0.10	0.02				5.5				
12	C614	Aluminum bronze-D	90.0	0.01		0.10	3.68				6.3				
13	C706	Cu:Ni (10%)	86.7	10.9		0.18	1.59								
14	C715	Cu:Ni (30%)	68.8	30.0		0.40	0.48	0.30							
15	C725	Cu:Ni:Sn	89.0	9.0	2.0										
16	C745	"Nickel–silver" 65-10	65.3	9.9		24.6									
17	C729	15-8 Spinodal	77.0	15.0	8.0										
18	C726	4-4 Spinodal	92.0	4.0	4.0										
19	N022	Comm. pure Ni	0.01	99.7			0.03	0.19					0.01		
20	A010	Commun. pure Al									99. min				

Table II. Sample Preparation Steps[a]

Grinding operations	Number of manual strokes
240	10
320	10
400	15
600	30
Polishing operations	
Compound	Comments
12-μm alumina	Remove 600 grit marks
6-μm diamond	Oil base on rayon
1-μm diamond	Oil Base on nylon
0.05-μm Cr/Ce oxide	Final polish, 1/2 hour on glocked twill

[a] Note that cleaning steps occur between each procedure.

ranged from 0.50 to 1.50 mm, while sheet sizes varied from 20 to 100 cm in overall dimensions. Care was taken to select nominally flat sheet specimens, which were then machined into 25.4-mm circular coupons by milling rather than punching to protect their central clear apertures of 12-mm diameter. Grinding operations consisting of a fixed number of strokes in four different directions (90 degrees apart) were performed on one face using wet 600-grit emery paper according to steps outlined in Table II. This was followed by mechanically polishing on a 12-μm alumina wheel to remove visual marks remaining from the emery paper. Then a 6-μm diamond polish was applied using rayon cloth to remove the 12-μm marks, which was followed by 1-μm diamond compound on a nylon cloth wheel. Finally, Syntron chromium cerium compound was used for approximately 0.5 h for each coupon for chemical polishing. Coupons were rinsed in pure distilled water, then blown dry with filtered nitrogen and stored in a desiccator jar until used individually in reported measurements. In all, this sample preparation procedure waqs found to produce repeatable results of optical absorptance measurements within the standard deviation of each measurement, which was repeated several times. Optical flatness was within half a wavelength for all polished faces.

5. DATA COLLECTION AND REDUCTION TECHNIQUE

The object of gathering data was to show a linear relationship between the absorbed fraction of laser power impinging on the target sample and

the amount of cooling required to offset this small heating effect. We therefore varied the incident laser power until low-level noise was exceeded but kept the maximum power level below the point where diffuse reflection became noticeable. These two limits were affected by drift in ambient room temperature at low power levels and by stray heating due to secondary reflections in the vacuum chamber at the highest diffuse reflection levels from the sample itself. A thermal sensor was connected to a perforated hemispherical cup placed over the specimen region as shown in Fig. 1. Whenever appreciable heating of this cup was observed, incident power from the laser was reduced to prevent heating. This precaution, plus placing an upper limit of approximately 800 mW delivered to the Peltier cooler, kept the absorbed laser power within a linear operating range for the apparatus used in this study.

Figure 2 shows a typical example of data gathered for a given sample. The input laser power values were selected by varying the optical attenuation in a stepwise fashion. Measured data were first recorded as a set of voltage values delivered to the Peltier cooler when thermal equilibrium was reestablished at each incident laser power setting. Then a calibration curve was used to compute the corresponding power to the Peltier cooler. These data, together with the corresponding laser input power setting for each trial, were fed to a table of values which served as input to a software program which computed a least-squares linear fit to experimental observa-

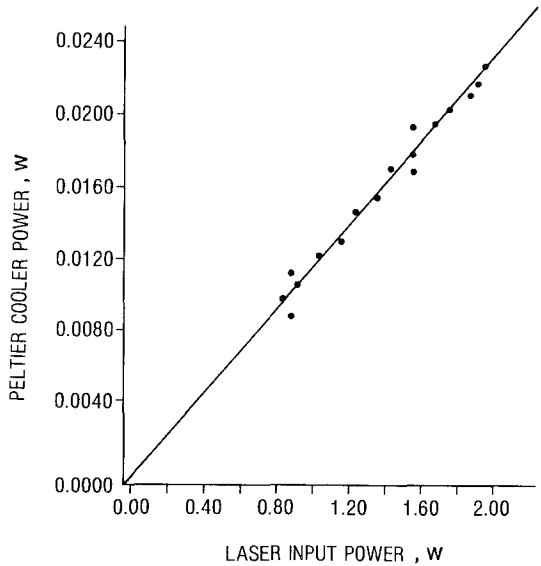

Fig. 2. Example of absorptance data measured for alloy C101 at a 10.6-μm wavelength.

tions. The program was constrained to force a straight-line fit throught the origin, since we required that aqll computations show no power delivered to the Peltier cooler in the absence of laser input. Computed slopes to a forced linear fit to all data then provided direct determination of absolute absorptance, together with computed standard deviation.

6. THEORETICAL CONSIDERATIONS

When an optical beam impinges upon a metallic surface, a portion of the beam is absorbed while the remainder is either specularly or diffusely relected. In simplest terms, the absorved portion A is related to unity incident intensity by

$$A = 1 - R \tag{1}$$

where R refers to the sum of both reflected contributions. At normal incidence, both A and R are related to the complex refractive index

$$\hat{n} = n + ik \tag{2}$$

by

$$A = 1 - R = \left|\frac{1-\hat{n}}{1+\hat{n}}\right|^2 = \frac{(1-n)^2 + k^2}{(1+n)^2 + k^2} \tag{3}$$

where n is the real part and k is the dissipation factor associated with $\hat{n}$. The simple Drude model of a metal considers the optical properties to be governed by free rather than bound charge carriers [1]. This means that the elastic constant K in the following charge displacement equation vanishes; i.e.,

$$m\ddot{x} + \gamma\dot{x} + Kx = E \sin \omega t \tag{4}$$

reduces to

$$m\ddot{x} + \gamma\dot{x} = E \sin \omega t \tag{5}$$

Starting with this expression and the simplified Drude model, we obtain

$$n^2 - k^2 = 1 - 2\left(\frac{Ne^2}{2\pi m^*}\right)\frac{1}{\nu^2 + \gamma^2} \tag{6}$$

$$nk = \frac{\gamma}{\nu}\left(\frac{Ne^2}{2\pi m^*}\right)\frac{1}{\nu^2 + \gamma^2} \tag{7}$$

$$\gamma = \left(\frac{Ne^2}{2\pi m^*}\right)\frac{1}{\sigma_{DC}} = \left(\frac{Ne^2}{2\pi m^*}\right)\rho_{DC} \tag{8}$$

where

$$N = \text{density of charge carriers}$$

$$e = \text{electron charge}$$

$$m^* = \text{effective electron mass}$$

$$\sigma_{DC} = \frac{1}{\rho_{DC}} = \text{DC conductivity}$$

$$\rho_{DC} = \text{DC resistivity}$$

In the range of λ from 1- to 10-μm infrared wavelengths, $k \gg n$, which permits us to write

$$\frac{k}{\lambda} = \sqrt{\frac{Ne^2}{\pi m^*}} \tag{9}$$

This leads to the following Hagen–Rubens expression [2] for absorptance:

$$A = 2\sqrt{\nu \rho_{DC}} \tag{10}$$

For most metals and alloys there is little agreement with such square-root dependency upon DC electrical resistivity. The later work of Reuter and Sondheimer [3] showed that at near-infrared frequencies, the absorptance behaves more like

$$A = 1 - R = \frac{c\rho_{DC}}{\pi} \tag{11}$$

with the prediction that A is closely proportional to the DC resistivity itself and tends to rise above the classical Drude value as the frequency is increased from very low values. For more complex alloys, there is little agreement over the dependency of A upon ρ_{DC} at the two wavelengths considered, but out data offer little more than a rank ordering for the copper-based alloys measured in our study.

7. DC RESISTIVITY MEASUREMENT

We used a four-point probe method to determine the DC resistivity of all sample coupons of copper-based alloy materials. This was done by means of a pulsed reversing DC current microohmmeter with a 0.100-in. probe spacing. All measurements were conducted on the optically poblished faces of the sample coupons near their centers after optical absorptance measurements had been completed. Accuracy of resistivity

measurements for the test apparatus has been independently shown [4] to lie within $\pm 3\%$ over a range of values from 1.7 to 200 $\mu\Omega \cdot$ cm.

The geometry of the samples measured corresponds to that of an infinite sheet of finite thickness. DC sheet resistivity is obtained [5].

$$\rho_{DC} = \left(\frac{V}{I}\frac{\pi}{\ln 2}\right) \quad \text{(thickness correction)} \tag{12}$$

$$\rho_{DC} = \left(\frac{V}{I}4.4324\right) F\left(\frac{W}{S}\right) \tag{13}$$

where

V = potential betweern inner probe points

I = injected probe current

S = separation between probe points

W = sample coupon thickness

Table III. Consolidated Results of Measurements

Sample No.	Alloy	Electrical resistivity ($\mu\Omega \cdot$ cm)	Optical absorptance at 1.06 μm	SD	Optical absorptance at 10.6 μm	SD
1	C101	1.81	0.0485	0.0019	0.0113	0.00015
2	C114	1.85	0.0500	0.0016	0.0103	0.00019
3	C112	2.17	0.0577	0.0016	0.0106	0.00026
4	C182	2.21	0.0448	0.0018	0.0120	0.00019
5	C230	4.83	0.0742	0.0035	0.0197	0.00026
6	C260	6.48	0.0672	0.0022	0.0239	0.00032
7	C443	7.66	0.0837	0.0036	0.0306	0.00034
8	C510	9.50	0.0809	0.0045	0.0289	0.00037
9	C521	15.8	0.0786	0.0047	0.0392	0.00022
10	C524	18.5	0.0907	0.0040	0.0456	0.00045
11	C608	10.5	0.111	0.0045	0.0351	0.00038
12	C614	14.7	0.0890	0.0030	0.0504	0.0013
13	C706	26.2	0.188	0.0085	0.0574	0.00097
14	C715	40.6	0.294	0.012	0.0786	0.0010
15	C725	18.3	0.166	0.0044	0.0344	0.0034
16	C745	20.8	0.206	0.0042	0.0534	0.0024
17	C729	30.0	0.124	0.0040	0.0890	0.00042
18	C726	11.9	0.220	0.0045	0.0579	0.00030
19	N022	9.25	0.267	0.0055	0.0282	0.00024
20	A0110	3.10	0.145	0.0051	0.0182	0.00015

The thickness correction function is described by Uhlir [6] and has been programmed into the apparatus microprocessor. Each sample thickness was carefully measured and entered into the "thickness calibration control" as an attenuation factor fed back into the probe monitor. Final DC resistivity values are listed in Table III for each sample tested.

8. RESULTS AND DISCUSSION

Principal findings of this study are shown in Table III, which lists results for each of 18 copper-based alloy types measured, plus additional samples of commercially pure nickel and aluminum. The common names of these materials are listed next to their unified code designations, followed by measured DC electrical resistivity and the values of optical absorptance measured at the two laser wavelengths of 1.06 and 10.6 μm, respectively. Each of the latter listings is following by computed values for the standard deviation derived from the least-squares fit to observations.

An average value of 3.8% was computed from the sum of all 20 values for standard deviation with respect to optical absorptance measured at a 1.06-μm wavelength, while an average value of 1.3% was computed from

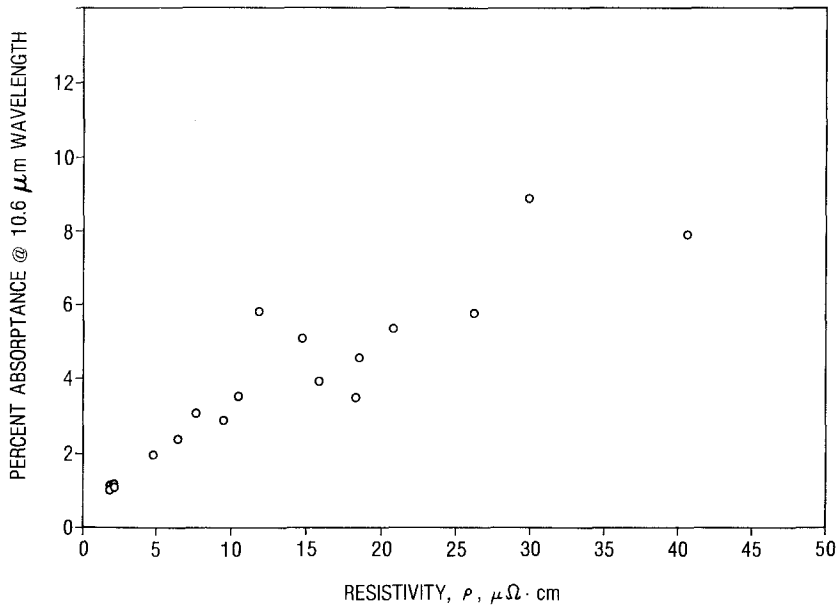

Fig. 3. Variation of absorptance with resistivity for copper-based alloys at a 1.06-μm wavelength.

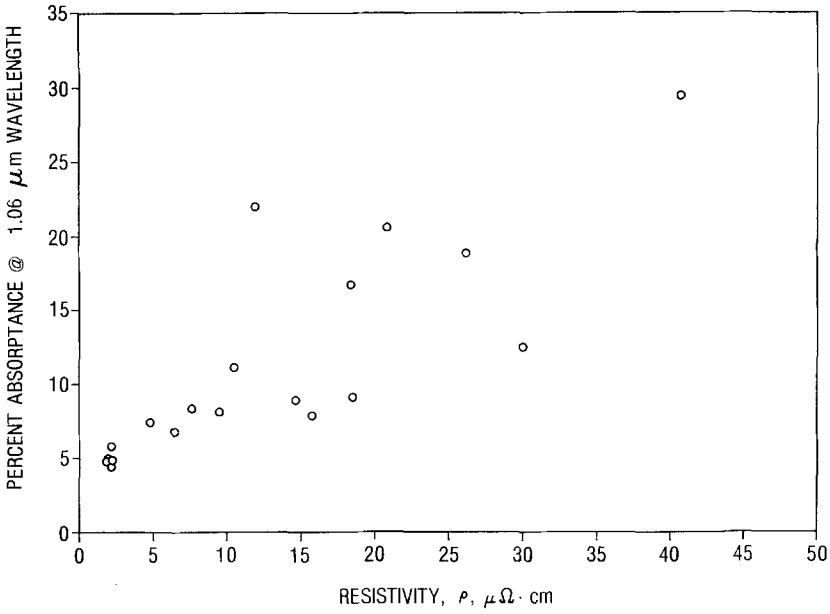

Fig. 4. Variation of absorptance with resistivity for copper-based alloys at a 10.6-μm wavelength.

the sum of all standard deviations at a 10.6-μm wavelength. This difference in precision between experimental determinations made at these two wavelengths is attributed to a noted difference in the temporal stability of the continuous power output of the two individual lasers used in this study. This is borne out by the claims of each manufacturer, in which the Nd:YAG laser has a stated long-term stability of approximately 5% or better, while that of the CO_2 laser is stated to be within 2%.

Examination of Figs. 3 and 4 reveals a roughly linear dependency between measured optical absorptance and DC electrical resistivity for the group of 18 copper-based alloys studied. While the correlation is considered poor, the plots do reveal a better fit at 10.6 μm than at 1.06 μm, as would be expected from theoretical considerations. However, only an ordered ranking of absorptance with respect to DC resistivity can be reported at this time.

9. CONCLUSION

A method has been described that permits direct measurement of optical absorptance for a metallic sample. An absolute determination of

the absorptance is found from a linear fit to the amount of cooling power delivered to a set of Peltier thermoelectric junctions as a function of incident laser power incident continuously upon the sample. Since this is an equilibrium measurement, totally independent of time, the precision of the method is based upon the maintenance of stability with respect to power delivered from the laser source, the sensitivity and ability of the temperature controller to track and maintain corrective current to the Peltier cooler, the preservation of the laboratory room temperature at a fixed ambient condition.

We have demonstrated that a laser-based method can achieve better than 5% accuracy with respect to measurement of absorptance for a wide range of copper-based alloys. While we attempted to provided each sample coupon with a high degree of optical polish and flatness, the method itself is amenable to absolute absorptance determination regardless of the surface condition.

While an attempt was made to compare measured values of near-infrared optical absorptance with DC electrical resistivity, only an ordered ranking was achieved. Such a comparison might yield more definitive results for a more restricted range of copper-based alloys and appears to deserve further investigation.

ACKNOWLEDGMENTS

The technical assistance of R. Borutta and R. J. Crisci in carrying out much of the experimental work reported is greatly appreciated.

REFERENCES

1. P. Drude, *The Theory of Optics* (Dover, New York, 1959), Chapter IV.
2. E. Hagen and H. Rubens, *Phil. Mag.* 7:157 (1904).
3. G. E. H. Reuter and E. H. Sondheimer, *Proc. Roy. Soc.* **A195**:336 (1948).
4. R. L. Cohen and K. W. West, *Mater. Eval.* **41**:1074 (1983).
5. F. M. Smits, *Bell Syst. Tech. J.* **37**:711 (1958).
6. A. Uhlir, Jr., *Bell Syst. Tech. J.* **34**:105 (195).